

# 1 **Komagataeibacter tool kit (KTK): a modular cloning system for multigene constructs and** 2 **programmed protein secretion from cellulose producing bacteria**

3

4 Vivianne J Goosens<sup>1,2</sup>, Kenneth T Walker<sup>1,2</sup>, Silvia M Aragon<sup>1,3</sup>, Amritpal Singh<sup>1,2</sup>, Vivek R Senthivel<sup>1,2</sup>, Linda  
5 Dekker<sup>1,2</sup>, Joaquin Caro-Astorga<sup>1,2</sup>, Marianne L A Buat<sup>2</sup>, Wenzhe Song<sup>4</sup>, Koon-Yang Lee<sup>4</sup> and Tom Ellis<sup>1,2</sup>

6

7 1. Imperial College Centre for Synthetic Biology, Imperial College London, London SW7 2AZ, UK

8 2. Department of Bioengineering, Imperial College London, London SW7 2AZ, UK

9 3. Department of Life Sciences, Imperial College London, London SW7 2AZ, UK

10 4. Department of Aeronautics, Imperial College London, London SW7 2AZ, UK

11

12 Correspondence to [t.ellis@imperial.ac.uk](mailto:t.ellis@imperial.ac.uk)

13

14 Bacteria proficient at producing cellulose are an attractive synthetic biology host for the emerging  
15 field of Engineered Living Materials (ELMs). Species from the *Komagataeibacter* genus produce high  
16 yields of pure cellulose materials in a short time with minimal resources, and pioneering work has  
17 shown that genetic engineering in these strains is possible and can be used to modify the material  
18 and its production. To accelerate synthetic biology progress in these bacteria, we introduce here  
19 the *Komagataeibacter* tool kit (KTK), a standardised modular cloning system based on Golden Gate  
20 DNA assembly that allows DNA parts to be combined to build complex multigene constructs  
21 expressed in bacteria from plasmids. Working in *Komagataeibacter rhaeticus*, we describe basic  
22 parts for this system, including promoters, fusion tags and reporter proteins, before showcasing  
23 how the assembly system enables more complex designs. Specifically, we use KTK cloning to  
24 reformat the *Escherichia coli* curli amyloid fibre system for functional expression in *K. rhaeticus*, and  
25 go on to modify it as a system for programming protein secretion from the cellulose producing  
26 bacteria. With this toolkit, we aim to accelerate modular synthetic biology in these bacteria, and  
27 enable more rapid progress in the emerging ELMs community.

## 28 **Introduction**

29

30 The emerging field of Engineered Living Materials (ELMs) uses synthetic biology to grow and  
31 engineer materials with characteristics that are prominent in nature, such as colour, self-repair,  
32 growth, conductivity and inherent sensing (Gilbert and Ellis, 2019; Tang et al., 2020). Being  
33 biological, these materials also remain biodegradable and can be grown from sustainable nutrient  
34 sources and so have great potential in a circular economy. A significant focus of early ELMs work  
35 has been on bacterial biofilms, and in particular, on manipulating proteinaceous amyloid fibres and  
36 cellulosic polymers as these lends themselves to a number of ELM-based applications (Gilbert and  
37 Ellis, 2019; Nguyen et al., 2018).

38 Bacterial cellulose (BC) is a a major component of biofilms and is unique in its purity,  
39 synthesis and network architecture, offering a biocompatible material with superior crystallinity and  
40 tensile strength compared to plant cellulose (Pallach et al., 2018; Yadav et al., 2010). These  
41 physiochemical characteristics of BC has made it valued in the food, beverage, cosmetic, surgical  
42 and biomedical industries and has enormous potential as an ELM (Gilbert and Ellis, 2019; Jang et al.,  
43 2017). Gram-negative acetic acid bacteria (AAB), in particular *Gluconacetobacter* and  
44 *Komagataeibacter* species, are prolific producers of BC.

45 In recent years, many advances have been made in molecular tools for the BC field (Florea  
46 et al., 2016; Gwon et al., 2019; Singh et al., 2020; Teh et al., 2019; Walker et al., 2018), however,  
47 both the general cellulose and the more specific cellulose-based ELM fields could greatly benefit  
48 from a Golden Gate (GG) cloning toolkit. Modular GG-based toolkits have revolutionised molecular  
49 and synthetic biology in other organisms including in yeasts, mammalian cells, plants, and gram-  
50 positive and gram-negative bacteria (Andreou and Nakayama, 2018; Engler et al., 2014; Hernanz-  
51 Koers et al., 2018; Iverson et al., 2016; Lee et al., 2015; Martella et al., 2017; Moore et al., 2016;  
52 Weber et al., 2011; Wicke et al., 2017). Toolkits with both broad or specific host-ranges, have been  
53 developed and are transforming their relevant fields (Chiasson et al., 2019; Geddes et al., 2019;  
54 Valenzuela-Ortega and French, 2019; Vasudevan et al., 2019; Wu et al., 2018). These cloning  
55 systems allow for rapid assembly of DNA constructs from modular genetic parts to build multigene  
56 systems. This is achieved using specially-designed complementary overhangs that are created by  
57 Type IIS restriction enzymes and joined by ligases.

58 Recognising a lack of such a system for BC-producing bacteria, we developed and herein  
59 describe the *Komagataeibacter* Tool Kit (KTK): a modular cloning system that caters to  
60 *Komagataeibacter* species, the BC biosynthesis field and those developing cellulose-based ELMs.

61 We define our KTK system and the plasmids and part standards associated with it, and then  
62 demonstrate its use in *Komagataeibacter rhaeticus*, a transformable native BC producer, in cases  
63 using basic parts for gene expression, and then for cases where multigene expression is necessary  
64 to achieve new functionality. As a case-study, we used KTK cloning to express *E. coli*'s Curli system,  
65 which produces the best-studied bacterial amyloid; a polymeric protein structurally rich in beta-  
66 sheets that forms a fibre with exceptional strength, stability and resistance (Evans and Chapman,  
67 2014). Curli has been a focus for many ELM-associated studies (Birnbaum et al., 2020; Chen et al.,  
68 2014; Nguyen et al., 2014; Seker et al., 2017), and offers promise for making a novel composite with  
69 BC in cells that can co-produce both materials. The Curli production system is also representative of  
70 a Type VIII secretion system (T8SS) and so its expression offers a tractable solution for protein  
71 secretion from BC-producing cells. Expressing this system in *K. rhaeticus* allows us to secrete Curli  
72 proteins and enzymes from BC-producing bacteria and demonstrates the power of the KTK system  
73 for assembling complex multigene modular assemblies.

74

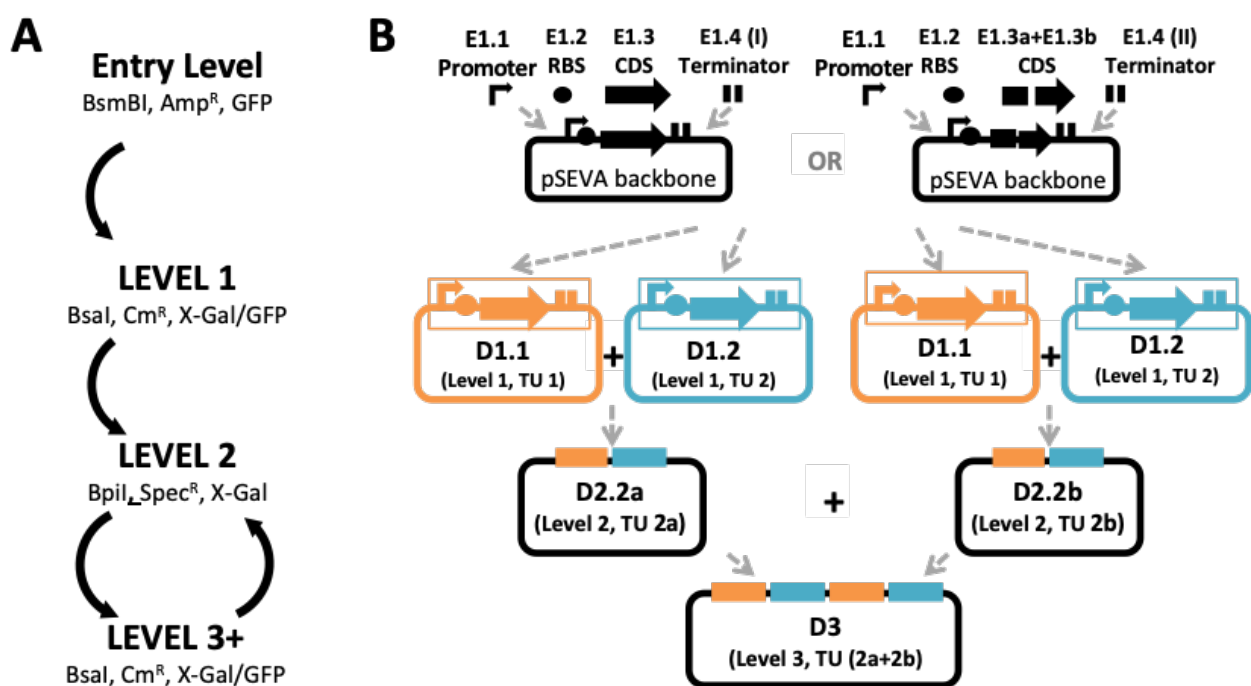
## 75 **Results**

### 76 **The Komagataeibacter Toolkit (KTK)**

77 The KTK system is an iterative, hierarchical Golden Gate (GG) cloning method best described in levels  
78 (**Fig 1a**). GG cloning takes advantage of Type IIS restriction enzymes (REs). These enzymes cut a short  
79 distance away from the recognition site to generate specific overhangs used for orientated ligations.  
80 Once these overhangs are joined, the DNA fragment no longer includes the initial RE site, thereby  
81 cementing the ligation and prevent re-cutting (for detailed guide and illustrations see  
82 **Supplementary Materials**). This GG system starts with *Entry-level Parts*, the basic DNA-encoded  
83 components required for gene expression in a single Transcriptional Unit (TU). Entry level parts  
84 include promoters (E1.1), a ribosome-binding site (RBS) sequences (E1.2), coding sequence (CDS)  
85 regions (E1.3) and terminators (E1.4) (**Fig 1b**). The Entry-level Parts are designed to include  
86 complementary GG overhangs for oriented ligations, so that when combined in the first level of  
87 cloning with a *Destination* vector backbone they ligate to form a plasmid with a single full  
88 Transcription Unit (**Fig 1b**).

89 KTK Destination Vectors are based on Standard European Vector Architecture (SEVA)  
90 plasmids, and benefit from the advantages of this powerful modular set (Durante-Rodríguez et al.,  
91 2014). The main destination vectors are adapted from the pSEVA331 and pSEVA431 plasmids, which  
92 have a pBBR1 replication origin and encode Chloramphenicol and Spectinomycin resistance  
93 markers, respectively. In the KTK system, the multiple cloning site (MCS) regions of these plasmids

94 has been modified to encode Golden Gate cloning sequences. A further possibility when  
 95 constructing a TU with KTK is to create a fusion protein in the CDS position (E1.3). The system allows  
 96 this by ligating C- and N-terminal domain CDS parts (E1.3a and E1.3b) (**Fig 1b**). The basic KTK system  
 97 includes a library of useful Entry-level Parts (promoters, RBS, terminators, and useful C- and N-  
 98 terminal CDS domains e.g. GFP, His-tag and signal peptides) as well as sequences that can be used  
 99 as 'spacers' that are useful at subsequent cloning levels. All plasmid construction is designed to be  
 100 done using *E. coli* cloning strains, before completed plasmids are then transformed into competent  
 101 *Komagataeibacter* for testing.  
 102



103  
 104 **Figure 1. The KTK cloning system.** (a) The levels of KTK cloning. Entry-level plasmids are ampicillin resistant  
 105 (Amp<sup>R</sup>), are selected by the absence of GFP, and BsmBI is used for cloning. In Level 1 (and Level 3) cloning  
 106 plasmids generated using BsaI, resulting in chloramphenicol resistant (Cm<sup>R</sup>) plasmids that have lost the X-Gal  
 107 or GFP marker cassette. BpiI is used in Level 2 cloning and resultant plasmids are spectinomycin resistant and  
 108 selected for by loss of X-Gal cassette. (b) Schematic of the Entry-level parts combining with a Level 1  
 109 backbone vector to form either a basic TU (made up of promoter (E1.1), RBS (E1.2) CDS (E1.3) and terminator  
 110 (E1.4I) parts or a fusion protein TU (made up of promoter (E1.1), RBS (E1.2), fused CDS (E1.3a +E1.3b) and  
 111 terminator (E1.4II) parts). There are two variations of Level 1 destination vectors and two variation of Level 2  
 112 destination vectors. Combined this allows the combination of 4 TUs at the 3<sup>rd</sup> cloning level. In both Level 1  
 113 and Level 2 cloning there are two possible destination vector backbones (D1.1 & D1.2 and D2.2a & D2.2b,  
 114 respectively). The 3<sup>rd</sup> cloning level recycles the same destination vectors as in Level 1, facilitating iterative  
 115 cycles of cloning between the two vector backbones.  
 116

117 For simple constitutive expression of a protein, constructing a TU via a single round of  
 118 cloning (level one) is sufficient. However, for multifaceted genetic constructs, such as inducible  
 119 expression cassettes or multi-part TUs, the KTK adds further cloning levels that enable versatile

120 construction. The backbone vectors for each cloning level have an alternating arrangement of  
121 flanking Type IIS RE sites (for BsaI and BpiI). These in turn generate specific overhangs that are used  
122 for the next level of cloning (illustrated and detailed in **Supplementary Materials**). The nature of  
123 Type IIS RE cloning means that one of set of RE sites are removed during the ligation reaction and  
124 the second set then becomes available for the next level of assembly. Furthermore, the KTK system  
125 provides two Backbone vectors for each cloning level, each with slight variation in overhangs to  
126 allow for the parallel insertion of different ligated DNA parts and TU assemblies. These can then be  
127 joined in the next level of ligation, thereby facilitating multiple cycles with multipart constructs (**Fig**  
128 **1b**).

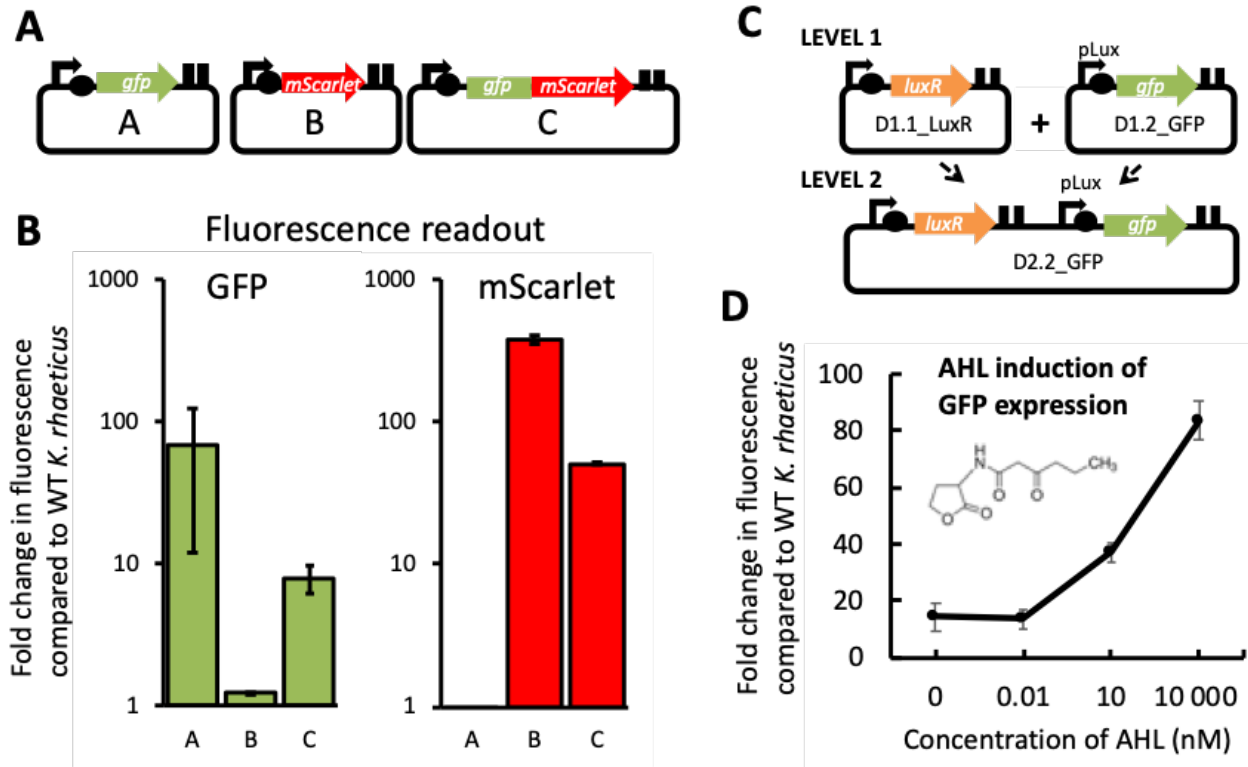
129

### 130 **Validating KTK Golden Gate cloning**

131 To validate Level 1 Golden Gate assembly with KTK, plasmids were constructed to express  
132 fluorescent proteins from encoded TUs. Entry-level Parts were first prepared, including the well-  
133 characterised constitutive promoter J23104 (E1.1) (Florea et al., 2016; Walker et al., 2018), a  
134 standard RBS (E1.2), a terminator (E1.4) and CDS parts (E1.3) encoding two fluorescent proteins,  
135 superfolder Green Fluorescent Protein (sfGFP) and mScarlet Red Fluorescent Protein (RFP). These  
136 two CDS parts were also cloned as N-terminal (E1.3a) and C-terminal (E1.3b) CDS parts to also allow  
137 assembly of a TU expressing sfGFP-mScarlet fusion protein (**Fig 2a**). Assembly of basic and fusion TU  
138 constructs was done using the KTK system with cloning steps in *E. coli*. The three constructs were  
139 then transformed into *K. rhaeticus* competent cells, and selected transformant colonies were then  
140 cultured in liquid growth media in the presence of purified cellulase (to prevent material formation)  
141 and measured for green and red fluorescence by flow cytometry (**Fig 2b**). The fluorescence intensity  
142 per cell compared to untransformed cells showed strong expression of both reporter proteins in  
143 basic TU form, and expression with reduced strength when constructed as a fusion protein.

144 Next, a multigene Level 2 construct was designed to yield a plasmid encoding externally-  
145 inducible GFP expression. Previous *K. rhaeticus* studies have taken advantage of the Vibrio Lux  
146 quorum sensing system for external gene expression induction (Florea et al., 2016; Teh et al., 2019;  
147 Walker et al., 2018). In the Lux system a regulator protein (LuxR) binds and induces expression of  
148 the gene coupled the pLux promoter when LuxR is bound to an acyl homoserine lactone (AHL). In  
149 the design chosen here, LuxR-AHL triggers expression of GFP. This two-gene construct was  
150 assembled by KTK cloning from Entry-level parts. Unlike in cloning of a single TU, choice of Level 1  
151 Destination vectors is important when going to Level 2. A TU constitutively expressing LuxR was

152 assembled into a D1.1 vector, while the TU expressing sfGFP from the pLux promoter was assembled  
 153 into a D1.2 vector (**Fig 2c**). The multigene Level 2 construct was then assembled from Level 1  
 154 constructs and transformed into *K. rhaeticus*. This construct worked as expected showing induction  
 155 of GFP expression in the presence of increasing AHL concentrations (**Fig 2d**).



156

157 **Figure 2. Validation of KTK cloning for basic TU and fused TU constructs (Level 1) and a multigene cassette**  
 158 **(Level 2).** (a) Design of the assembled fluorescent protein expressing constructs used to validate KTK level 1  
 159 cloning. All promoters used are J23104. (b) Fluorescence per cell measured by flow cytometry of *K. rhaeticus*  
 160 strains expressing GFP, mScarlet or a fused GFP-mScarlet protein. Values normalised to untransformed *K.*  
 161 *rhaeticus* with GFP fluorescence shown in green and mScarlet in red. Error bars represent SD of three  
 162 replicates. (c) Cloning schematic showing the use of different Destination vectors to enable Level 1 to Level  
 163 2 cloning. Level 1 assembly results in a LuxR-expressing TU (with J23104 promoter), and a TU with pLux  
 164 promoter and GFP. Level 2 cloning brings these TUs together to give an AHL-inducible GFP expressing  
 165 plasmid. (d) *K. rhaeticus* strains with the plasmid constructed in (c) were exposed to a range of exogenous  
 166 AHL concentrations in liquid growth phase and GFP fluorescence per cell was measured by flow cytometry.  
 167 Error bars represent SD of three replicates.

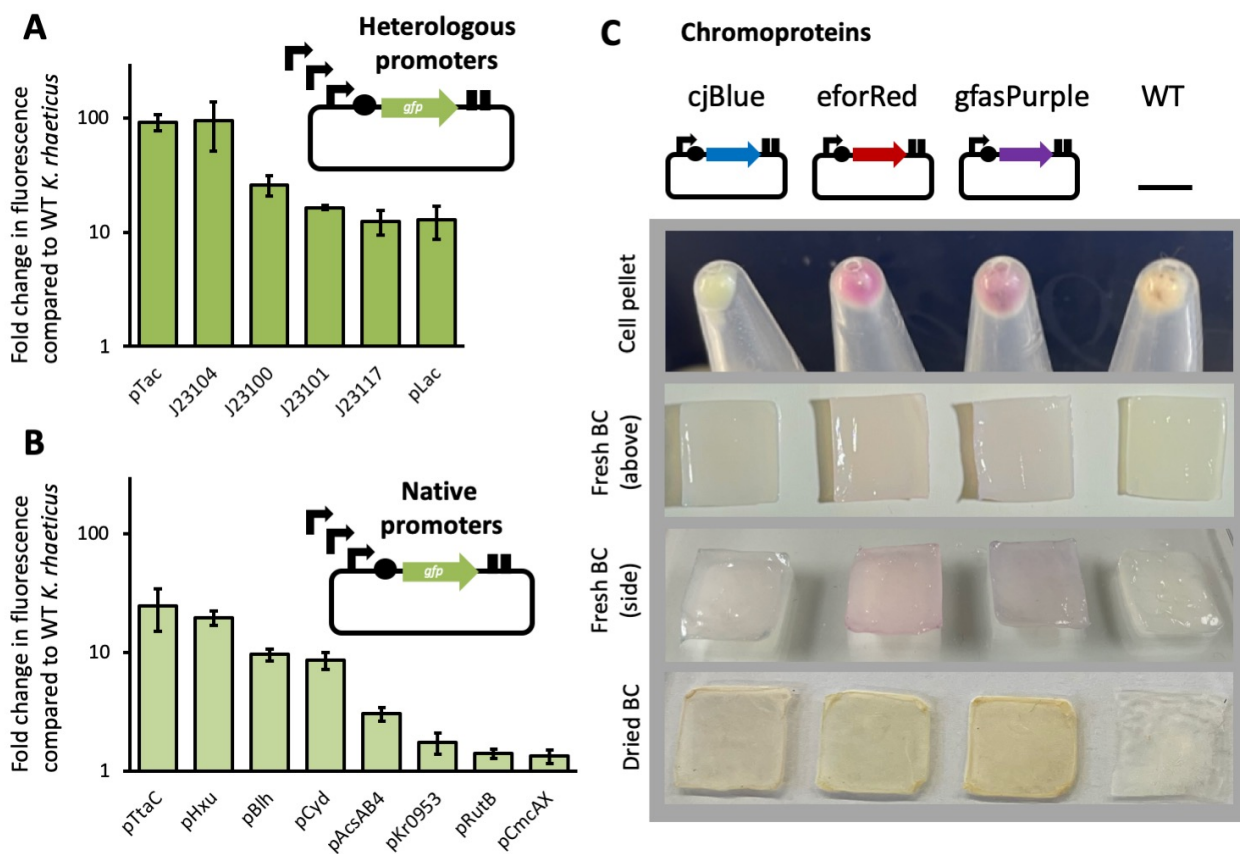
168

### 169 Expanding and characterising the KTK parts library

170 The utility of GG-based cloning toolkits are dependent on the size, characterization and availability  
 171 its Parts. To populate the KTK system we prepared a library of shareable Entry-Level Parts as well as  
 172 useful Destination-Level plasmids (**Table S1**). This library includes a panel of promoters, RBS  
 173 sequences, terminators, and basic CDS parts (selection cassettes, fluorescent proteins) as well as  
 174 spacer sequences that enable more complex assembly steps. Our basic library will be made available  
 175 to researchers and is intended to become a resource for the wider community.



176 As tuning gene expression is a key goal in engineering cells, we characterised a panel of  
 177 promoters including heterologous promoters and promoters native to *K. rhaeticus*, with the latter  
 178 identified from genes and operons known to express from the strain genome. KTK enabled  
 179 straightforward and quick assembly of modular constructs expressing sfGFP in basic TUs, each with  
 180 a different promoter. These promoters were then characterised for expression strength in liquid  
 181 growth phase using flow cytometry quantification of green fluorescence. J23104 and pTac  
 182 promoters were the strongest heterologous promoters (**Fig 3a**), while the native promoters pTtcA  
 183 and pHxu were the strongest of the ones taken from the genome sequence (**Fig 3b**). The individual  
 184 strengths of the heterologous promoters in KTK format correlate well to their strengths measured  
 185 in past work in this strain in different DNA formats (Florea et al., 2016; Teh et al., 2019).



186  
 187  
 188 **Figure 3. Characterization of promoters for the KTK parts library.** (a) Fluorescence per cell measured by flow  
 189 cytometry of *K. rhaeticus* strains expressing GFP in a standard single TU from 6 different heterologous  
 190 promoters. (b) Fluorescence per cell measured by flow cytometry of *K. rhaeticus* strains expressing GFP in a  
 191 standard single TU from 8 native promoters. Values in the plots are normalised to untransformed *K.*  
 192 *rhaeticus*. Error bars represent SD of three replicates. (c) Cell pellets (top row), fresh BC pellicles (middle two  
 193 rows) and air-dried BC pellicles (bottom) from cells transformed with plasmids expressing 3 representative  
 194 chromoprotein reporters.

195

196 We further sought to add reporter proteins visible to the naked eye that can be expressed  
197 within cellulose materials. To this end, we cloned 3 chromoproteins previously characterised in *E.*  
198 *coli* (Liljeruhm et al., 2018) that are visibly blue (cjBlue), red (eforRed) and purple (gfasPurple). When  
199 expressed in *K. rhaeticus* as a level 1 construct with J23104 promoter, each chromoprotein was able  
200 to change the colour of the bacterial cell pellet (**Fig 3b**), although cjBlue gave a more greenish hue  
201 than expected. The resulting bacterial cellulose pellicles grown from these strains showed visible  
202 colouration of the material, with the red and purple colours being particularly striking. However, on  
203 dehydration of the cellulose, pigmentation was lost, although the final material was still notably a  
204 different shade to cellulose made from unmodified cells (**Fig 3b, Fig S3**).

205 The basic KTK parts library contains several reporter proteins, terminators, RBS sequences and  
206 constitutive promoters, as well as the AHL-inducible promoter (**Fig 2**). We aim to expand this soon  
207 to include more inducible expression systems and constructs that allow for CRISPR-based gene  
208 regulation, and share the most relevant plasmids as a distributable collection.

209

#### 210 **KTK construction of an inducible curli system**

211 For a case-study application of the KTK system, we next designed and constructed a multigene  
212 assembly to express and extrude curli amyloid fibres from *K. rhaeticus*. In *E. coli*, curli fibres are  
213 polymerised on the outer surface of the cell from monomers of the CsgA protein, with this facilitated  
214 by five other curli proteins that act to chaperone (CsgC) and nucleate (CsgB) fibre formation, and  
215 form a curli-specific type VIII secretion system (T8SS) (CsgE, CsgF, CsgG) through the outer  
216 membrane (Evans and Chapman, 2014; Van Gerven et al., 2015) (**Fig 4A**). In *E. coli* these genes are  
217 encoded on two divergent operons, however a number of landmark ELM studies have elegantly  
218 functionalised curli by rearranging these genes into an easier-to-engineer synthetic linear operon  
219 (Kan et al., 2019). The linear operon format enables researchers to more readily modify curli through  
220 C-terminal CsgA fusions (small peptides or whole proteins) or by exploiting the signal peptide (the  
221 first 22 amino acids of CsgA) to secrete heterologous proteins through the Curli T8SS (Assalkhou et  
222 al., 2007; Birnbaum et al., 2020; Botyanszki et al., 2015; Nguyen et al., 2014; Nussbaumer et al.,  
223 2017; Seker et al., 2017; Sivanathan and Hochschild, 2012; Tay et al., 2017; Van Gerven et al., 2014;  
224 Wang et al., 2017; Zhong et al., 2014).

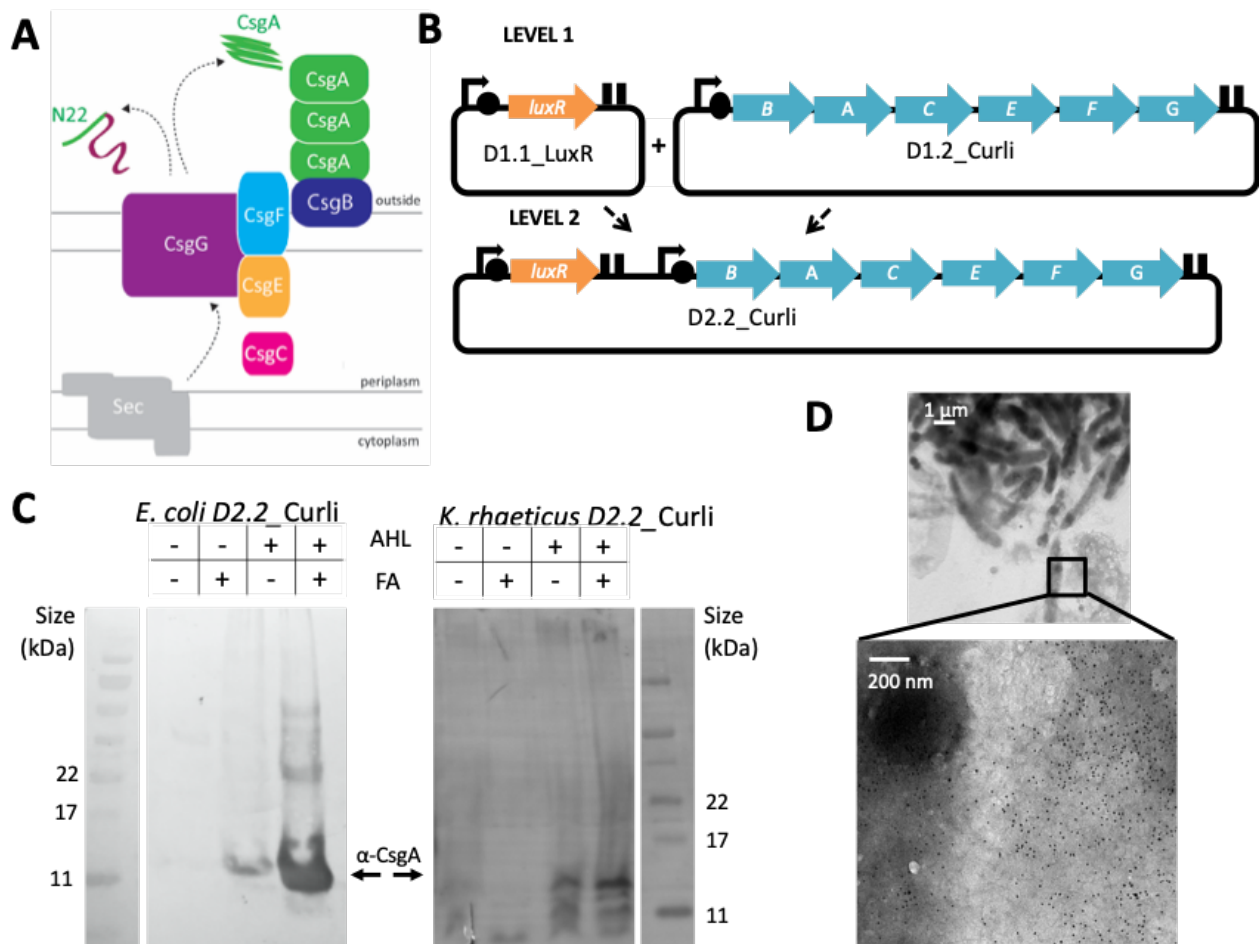
225 To port the *E. coli* curli system into BC-producing bacteria, we chose to maintain the linear  
226 operon format successfully employed in past ELMs work. The region encoding the 6 genes from the  
227 synthetic *E. coli* operon was therefore cloned into a KTK Entry-level vector as if it was a single CDS



228 (E1.3) part (**Fig 4B**). This was then assembled into a Level 1 curli-containing plasmid (D1.2\_Curli),  
229 with the AHL-inducible pLux promoter (E1.1), a well-characterised terminator (E1.4I) and an RBS  
230 (E1.2) part, selected by the RBS Calculator (Salis et al., 2009) to give a similar predicted strength for  
231 CsgB translation as that seen in the native *E. coli* system. D1.2\_Curli was then assembled with a  
232 Level 1 LuxR-expressing plasmid (D1.1\_LuxR) to create the multigene Level 2 plasmid construct  
233 giving AHL-inducible Curli expression (D2.2\_Curli). In this design LuxR is expressed by a medium  
234 strength promoter (pLac) to reduce any potential burden.

235 As KTK constructs are compatible in *E. coli*, assays for plasmid function can be performed in  
236 *K. rhaeticus* and *E. coli* in parallel. To test for expression and production of CsgA from the D2.2\_Curli  
237 construct, we first used Western blot analysis. As amyloid fibres are resistant to heat and  
238 detergents, formic acid (FA) treatment is required for depolymerisation SDS-PAGE separation of  
239 CsgA and so can be used to identify if the CsgA is polymerised or just in monomeric form. Protein  
240 extracts taken from uninduced or AHL-induced *K. rhaeticus* and *E. coli* were separated and stained  
241 (**Fig 4c**) for monomeric CsgA (visible band with no FA treatment) and polymeric CsgA (visible band  
242 only seen with FA treatment), confirming that the D2.2\_Curli construct produced CsgA and  
243 polymerised it into curli fibres in both *K. rhaeticus* and *E. coli*.

244 Transmission electron microscopy (TEM) was next performed to visualise curli fibre  
245 production from transformed *K. rhaeticus*. As control, TEM analysis of AHL-induced *E. coli* showed  
246 clear filamentous Curli structures (**Fig S1a**) confirming the plasmid function in this bacterium. Direct  
247 visualisation was more challenging with *K. rhaeticus* due to cellulose fibres being present in large  
248 amounts, even after 20% (w/v) cellulase treatment (**Fig S1b**). Therefore, to distinguish curli from  
249 cellulose, TEM samples were treated with CsgA-polyclonal antibody and immunogold-labelled. Gold  
250 nanoparticle staining was evident in a tangle of fibres outside the *K. rhaeticus* cell, demonstrating  
251 that the plasmid is functional in the cellulose-producing bacterium (**Fig 4D and Fig S1b**). The effect  
252 of induced co-production of curli on the material properties of grown bacterial cellulose was then  
253 investigated to see if this cellulose-amyloid composite had greater strength than cellulose alone.  
254 Strength tests were performed on pellicles grown from AHL-induced *K. rhaeticus* with the D2.2\_Curli  
255 construct (**Fig S1c**). Pellicles grown from cells containing the D2.2\_GFP construct were used as a  
256 comparable control. No significant difference in strength was observed between the control and  
257 curli-positive pellicles, likely due to a very low relative abundance of curli compared to cellulose in  
258 the final material.



259

260 **Figure 4. Expressing an inducible Curli system in *K. rhaeticus*** (a) Schematic of the *E. coli* curli system where  
 261 amyloid fibres are assembled composed of polymers of CsgA, nucleated to the cell surface via CsgB. These  
 262 proteins are chaperoned (CsgC) and transferred over the outer membrane via a specialised Type VIII  
 263 secretion (T8S) system (CsgE, CsgF, CsgG). All proteins are secreted into the periplasm via the Sec system,  
 264 however, the N22 region of CsgA (shown in green) is essential for directing the protein through the CsgG  
 265 pore in the outer membrane. (b) Cloning schematic illustrating the KTK assembly of the AHL-inducible, Curli-  
 266 expressing D2.2\_Curli plasmid from two level 1 plasmids. (c) Western blot of protein extractions from *E. coli*  
 267 and *K. rhaeticus* cultures transformed with the D2.2\_Curli plasmids. Cultures were grown with or without  
 268 AHL inducer and obtained extracts were treated with or without Formic Acid (FA) to denature Curli proteins.  
 269 Polyclonal anti-CsgA antibody was used for detection and the CsgA band is indicated with an arrow. (d)  
 270 Transmission electron microscopy visualisation of gold particle-stained curli proteins outside of a D2.2\_Curli  
 271 expressing *K. rhaeticus* (inset). Black dots in the high magnification image are gold nanoparticles bound to  
 272 the curli protein via  $\alpha$ -CsgA rabbit antibody and 10 nm anti-rabbit IgG-Gold coupled antibody.  
 273

#### 274 **Programming protein secretion via the Type VIII secretion system**

275 For an example of a Level 3 KTK multigene assembly, we next constructed a plasmid that exploits  
 276 the curli-specific T8SS system for heterologous protein secretion (Fig 5a). Previous studies have  
 277 shown that the first 22 amino acids (N22) of CsgA are enough to target small heterologous proteins  
 278 for secretion via T8SS (Sivanathan and Hochschild, 2012; Wang et al., 2017). To make use of this we  
 279 split the curli operon into modules, with the 3 genes encoding the T8SS (CsgE, CsgF, CsgG) as a key  
 280 part and the N22 signal used as a tag to be fused to proteins for secretion (Fig 5a).

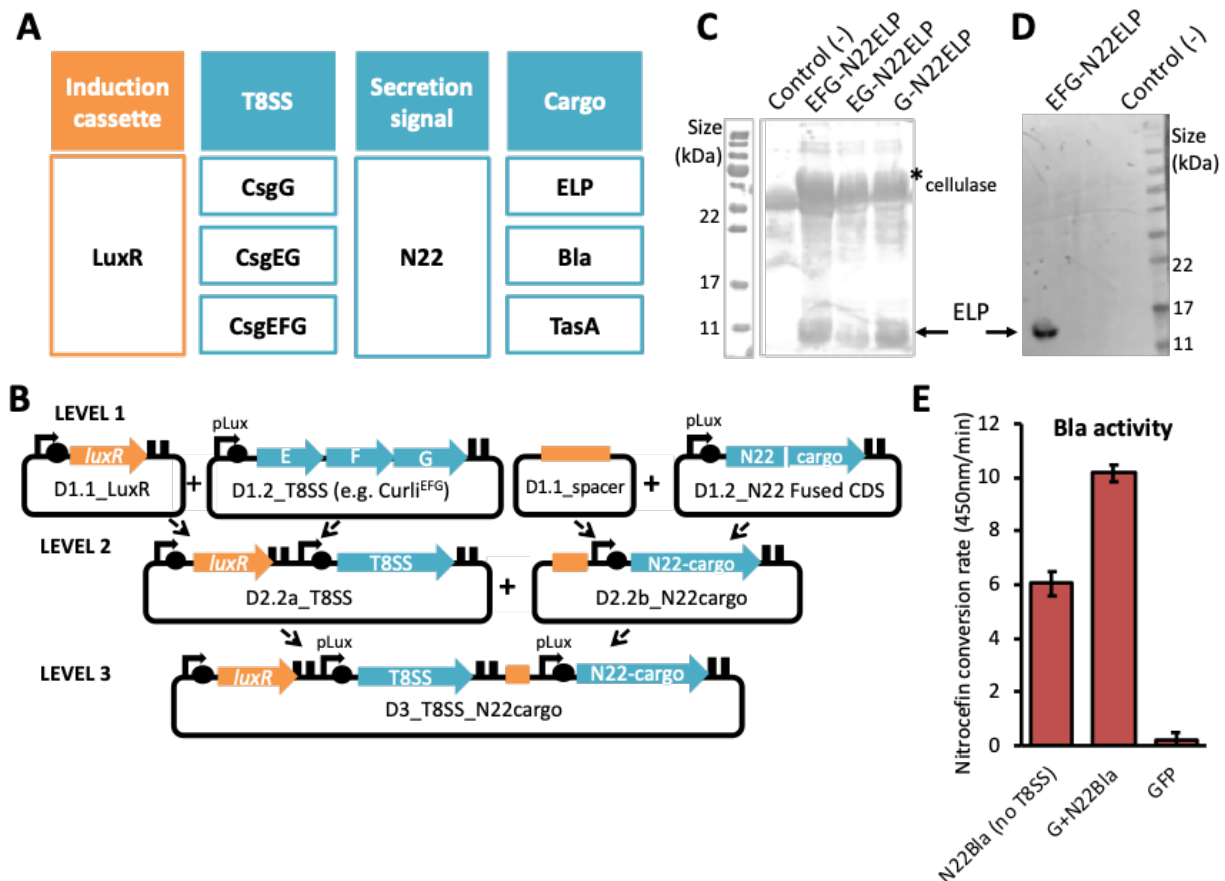
281 A panel of three T8SS modules were cloned into KTK as CDS parts; the minimal T8SS (just the  
282 secretion pore CsgG), CsgG plus the CsgE ‘adapter protein’ (CsgGE), and both of these proteins plus  
283 secretion chaperon CsgF (CsgEFG) (Costa et al., 2015; Hospenthal et al., 2017). These were  
284 assembled to Level 2 with a LuxR TU, so that expression of these T8SS modules was AHL-dependent  
285 (**Fig 5b**). In parallel, a small panel of heterologous cargo targets were prepared using the 2-part CDS  
286 fusion approach of KTK to bring together the N-terminal N22 region of CsgA (E1.3a part) with C-  
287 terminal CDS parts (E1.3b) encoding three targets: a 98 amino acid elastin-like protein (ELP), the  
288 enzyme Beta-lactamase (Bla) and the Gram-positive amyloid protein TasA (**Fig 5a-b**). ELPs are small  
289 unstructured versatile proteins that are highly hydrophobic and an attractive ELM component  
290 (Roberts et al., 2015), Beta-lactamase is a classic enzyme easily detected by the colorimetric  
291 nitrocefin assay (Gilbert et al., 2021), and TasA is an amyloid protein from *B. subtilis* that could be  
292 an alternative to curli (Erskine et al., 2018).

293 The 3 heterologous cargo targets were assembled into a Level 1 TU construct with the pLux  
294 promoter, before then being each combined into a Level 2 construct with a short spacer part  
295 (D1.2\_Spacer, 23 bp) designed to assist cloning of an odd number of TUs in a multigene assembly  
296 (**Fig 5b**). With all modules now in place in Level 2 plasmids, a combinatorial set of nine possible Level  
297 3 constructs could be assembled with the 3 different T8SS versions and 3 cargo proteins (**Fig 5a**).

298 To test the function of these constructs, we again performed experiments in parallel in *E.*  
299 *coli* and *K. rhaeticus* transformed with constructs, culturing with AHL induction and then harvesting  
300 in mid-log growth phase and separating supernatant and cell fractions. We first assessed ELP  
301 expression and secretion, using SDS-PAGE of both *K. rhaeticus* (**Fig 5c**) and *E. coli* (**Fig S2a**) samples  
302 to confirm the presence of processed and secreted ELP when any one of three T8SS versions were  
303 present. As ELP proteins are difficult to transfer by Western Blot due to their hydrophobic nature,  
304 the constructs were designed to include a C-terminal his-tag. This enabled us to identify that the 10  
305 kDa protein observed in the secreted fraction was indeed ELP-his when either *K. rhaeticus* (**Fig 5d**)  
306 or *E. coli* (**Fig S2b**) were expressing the CsgEFG T8SS constructs. Similar experiments with the TasA  
307 cargo were not as successful, only showing a small amount of TasA in cell fractions of *E. coli* (**Fig**  
308 **S2c**), suggesting that TasA cannot use the curli T8SS for export.

309 Finally, we assessed enzyme secretion from the beta-lactamase (Bla) encoding Level 3  
310 constructs, as before testing in both *E. coli* and *K. rhaeticus*. Beta-lactamase converts nitrocefin from  
311 a yellow to red colour, which is quantifiable by spectroscopy at 450nm and initial *E. coli* data showed  
312 that in the presence of either T8SS version, Bla enzymatic activity in the supernatant was higher  
313 than when no T8SS was present (**Fig. S2d**). In this case the minimal T8SS (CsgG) gave the highest

314 values, so the Level 3 construct expressing this with N22-Blac was then assessed in *K. rhaeticus*.  
 315 Supernatant from an AHL-induced culture of these bacteria showed beta-lactamase activity nearly  
 316 2-fold higher than when no T8SS is expressed in the cells (**Fig 5d**). Altogether the results with ELP  
 317 and Bla cargos show that the modular T8SS system generated here for the KTK system can be used  
 318 to program protein secretion from *K. rhaeticus*. Further work is needed to understand the optimal  
 319 T8SS version, its ideal expression level and what design considerations are needed for protein cargos  
 320 and their secretion.



321

322 **Figure 5. Using a T8SS module to secrete heterologous cargo proteins** (a) Modular components of the KTK-  
 323 based T8SS constructs. The first module (orange) represents the induction cassette (LuxR) for controlling  
 324 gene expression, further modules (teal) are 3 versions of the T8SS (CsgG, CsgEG and CsgEFG), the secretion  
 325 signal (N22) and the heterologous cargo proteins (ELP, Bla and TasA). (b) Cloning schematic to generate an  
 326 AHL-inducible modularised T8SS for heterologous protein secretion using the KTK system. Four level 1  
 327 constructs are made: an induction cassette construct (D1.1), the secretion system construct (D1.2), a spacer  
 328 construct (D1.1) and constructs that fuse the secretion signal (N22 sequence) to the cargo protein (D1.2).  
 329 These are combined in pairs to level 2 into the D2.2a and D2.2b vectors. A final assembly creates the Level 3  
 330 construct, D3\_T8SS\_N22cargo, which contains both an inducible secretion target and secretion system. (c)  
 331 SDS-PAGE (left) and Western Blot (right) of samples extracted from culture supernatants from AHL-induced  
 332 *K. rhaeticus* strains expressing a T8SS module (CsgEFG, CsgEG and CsgG) and N22-ELP-his. To aid liquid phase  
 333 growth and remove cellulose material, exogenous purified cellulase was added to the cultures and is clearly  
 334 visible in the SDS-PAGE protein gel. (d) Nitrocefin assay measuring the Beta-lactamase (Bla) activity of  
 335 supernatant harvested from an induced *K. rhaeticus* strain designed to express CsgG and N22-Bla. An  
 336 inducible strain expressing GFP (D2.2\_GFP) was used as a negative control in this experiment. Error bars  
 337 represent SD of three replicates.

## 338 Conclusion

339 Through a standardised hierarchical Golden Gate DNA assembly approach, the KTK system allows  
340 modular construction of single genes and multigene systems for cellulose-producing  
341 *Komagataeibacter*. We here validated this toolkit using fluorescent protein and chromoprotein  
342 constructs, before applying it to the modular construction of plasmids that enable inducible  
343 production of curli fibres by *K. rhaeticus* and heterologous protein secretion by this strain. These  
344 examples demonstrate the power of the combinatorial and modular toolkit system.

345 We provide a selection of basic parts along with the KTK system for tuning, controlling and  
346 measuring gene expression. Using promoters and RBS parts of different strength is a powerful way  
347 to optimise gene function in bacteria. Most of the experimental results shown here were done  
348 without any optimisation of expression of assembled genes. Design-led or combinatorial  
349 approaches choosing from promoter and RBS libraries are likely to be able to improve on the results  
350 seen here for the various demonstrations, for example in helping to make an updated GFP-RFP  
351 fusion construct (**Fig 2c**) that maintains equivalent fluorescence to constructs expressing only one  
352 of the two proteins.

353 To demonstrate how multigene assembly with the KTK system can advance engineered living  
354 materials, we imported the well-studied *E. coli* curli fibre production system into KTK and used it to  
355 engineer a construct that instructs *K. rhaeticus* to co-secrete curli fibres alongside cellulose as  
356 material is produced. Although KTK-based cloning was successful in enabling the production of  
357 amyloid curli outside the cell, this did not result in any marked change in material properties for the  
358 cellulose-curli composite pellicle. This is likely due to relatively very low production of protein  
359 compared to cellulose from these bacteria, or could be related to curli fibre formation being  
360 impaired chemically by the low pH of *K. rhaeticus* cultures, or physically by the large amounts of  
361 cellulose being extruded from the cell surface. In future work, curli production could be improved  
362 by increasing gene expression with different promoter/RBS parts and by using alternative gene  
363 arrangements, *e.g.* by using strong promoters and a two-module design (Bongers et al., 2005;  
364 Mierau et al., 2005; Tabor, 1990).

365 The potential of the curli system was further exploited here by taking advantage of its Type  
366 VII secretion system (T8SS) to export heterologous cargo proteins. An N-terminal fused N22 region  
367 from CsgA enabled secretion of a small unstructured ELP proteins when expressed in cells co-  
368 expressing the CsgEFG T8SS. The tag also gave promising results with Bla for the secretion of active  
369 globular enzymes from *K. rhaeticus* strains expressing CsgG. This offers the first described route to  
370 getting enzymes expressed in BC-producing bacteria to be secreted extracellularly, opening up the

371 possibility of having cellulose-binding or cellulose-modifying enzymes co-produced as the cellulose  
372 material is grown. However, the relatively low levels of protein and enzyme activity observed, and  
373 the failure to secrete TasA here suggests that achieving high-level programmed secretion of a  
374 desired target protein will more often than not be a challenge and will likely to require significant  
375 optimisation. We hope that many people will use and contribute to the KTK system in the future, to  
376 add more genetic parts that enable rapid optimisation of constructs in BC-producing bacteria. The  
377 parts and toolkit described here and in the supplementary materials currently remain untested in  
378 other BC-producing strains but we are optimistic that they will work well in all *Komagataeibacter*  
379 and other acetobacter. Indeed modular DNA parts developed previously by us and others for *K.*  
380 *rhaeticus* have been shown to be functional in *Gluconacetobacter xylinus* and *Gluconacetobacter*  
381 *hansenii* (Florea et al., 2016; Gwon et al., 2019; Singh et al., 2020; Teh et al., 2019; Walker et al.,  
382 2018). Parts from these past publications, including promoters, RBS sequences and CRISPR-derived  
383 gene regulation tools, can presumably be reformatted to work within our KTK system. We look  
384 forward to many interesting and innovative genetic parts being added to this toolkit as the growing  
385 community in synthetic biology and material sciences begin to produce BC-based ELMs with new  
386 functionalities and diverse and exciting properties.

387



## 388 **Materials and Methods**

### 389 **Strains and culture conditions**

390 The *E. coli* Turbo (NEB) was used throughout this study. Cultures were grown at 37 °C in shaking  
391 liquid Lysogeny Broth (LB) (10 g/l Tryptone, 5 g/l Yeast Extract, 5 g/l NaCl) or on LB agar (1% agar),  
392 and when appropriate supplemented with ampicillin (100 µg/ml), chloramphenicol (34 µg/ml) or  
393 spectinomycin (100 µg/ml). Transformation was done using chemically competent cells.

394 *K. rhaeticus* iGEM cultures were grown at 30°C in liquid Hestrin–Schramm media (HS) (2%  
395 glucose, 10 g/l yeast extract, 10 g/l peptone, 2.7 g/l Na<sub>2</sub>HPO<sub>4</sub> and 1.3 g/l citric acid, pH 5.6–5.8) or  
396 on HS agar plates (1.5% agar). When growing shaking cultures the media was supplemented with  
397 2% cellulase (Sigma Alrich, C2730) and, when appropriate, supplemented with chloramphenicol (34  
398 µg/ml) or spectinomycin (100 µg/ml). Electroporation of *K. rhaeticus* strains was performed as  
399 described previously (Florea et al., 2016), and transformants screened on 10x Chloramphenicol (340  
400 µg/ml) or 5x spectinomycin HS plates (500 µg/ml). When preparing pellicles for strength tests, *K.*  
401 *rhaeticus* was strains were firstly grown to high density in liquid in the presence of 1x antibiotic. This  
402 was then washed twice with HS media, resuspended in fresh cellulose-free HS media to a density of  
403 0.5 OD<sub>600</sub>. This density was also used as standard for pellicle inoculums. Pellicles were grown  
404 stationary at 30°C in fresh cellulase free HS media (75-100 ml), supplemented with antibiotic, and  
405 when appropriate 50 mM AHL. Thick pellicles were observed and harvested after 2-4 weeks.

406

### 407 **Molecular techniques, primers and plasmids**

408 Modular DNA parts and plasmids used and constructed in this study are listed in Supplementary  
409 Table S1 and S2. Standard PCR or primer joining was used to generate the DNA fragments for the  
410 entry-level parts. PCR was performed by standard protocol using a high-fidelity polymerase as per  
411 manufacturer's instructions. Primers are designed to include BsmBI and BsaI required for cloning as  
412 detailed in sequences shown in Table G1 and Figure G1. If Entry-level parts were small (<60 bp),  
413 instead of a PCR reaction, a primer joining protocol was used. Each primer would cover the target  
414 sequence and including the overhang and RE sites detailed in Table G1 and Figure G1. In order to  
415 allow primers to anneal together a sequence of overlap of at least 15 bp is required. Oligos (100 µM)  
416 are separately phosphorylated with T4 PNK (NEB) before combined and heated to 96°C for 6 min.  
417 Samples are annealed by ramping down to 0.1°C per second till 23°C. 10 µl of the mixture was used  
418 to clone into the Entry-Level Backbone vectors.

419 Golden Gate (GG) assembly followed standard GG protocols published (Lee et al., 2015).  
420 Briefly T4 DNA Ligase (Promega, C1263), T4 ligase (0.5 µl; NEB, M0202), Type IIs RE (0.5 µl, NEB),

421 vector backbone and inserts were combined to make 10  $\mu$ l. For optimum results a ratio of insert to  
422 backbone of 1:2 was used, *ie.* 50 fmol/ $\mu$ l per insert to 25 fmol/ $\mu$ l of backbone. Thermocyclers were  
423 used for assembly with 25 cycles of digestion at 42 °C (2 min) and ligation (16°C, 5 min), before two  
424 heat inactivation steps at 60°C (10 min) and 60°C (10 min). After which DNA was be transformed as  
425 per standard protocols and plated on prepared selectable plates.

426 Although GG was used primarily, Gibson cloning was required to adapt more complex entry-  
427 level parts, specifically the removal of BsaI restriction enzyme site from the CsgB gene in the  
428 synthetic Curli operon, and when building the CsgE-CsgG operon. All Entry-level vectors were  
429 sequenced and subsequent plasmids were confirmed with overlapping PCR to ensure all the  
430 fragments were present and had combined correctly.

431

### 432 **AHL induction assays**

433 For protein expression assays both *E. coli* and *K. rhaeticus* cultures were grown shaking to mid  
434 exponential phase. Cells treated with 50 nM (*E. coli*) or 50  $\mu$ M (*K. rhaeticus*) of AHL (N-Acyl  
435 homoserine lactone, Sigma-Aldridge K3255) and induced for approximately 4 doubling times (*i.e.* 2  
436 hrs or 16 hrs respectively). Cells were harvested and corrected for by OD<sub>600</sub> before further analysis  
437 performed.

438

### 439 **Chromoprotein expression**

440 *K. rhaeticus* starter cultures were grown in HS-glucose media with chloramphenicol antibiotic at 35  
441  $\mu$ g/mL for 3 days prior to inoculation of 5 mL of HS-glucose in 24-well deep well plates. The plate  
442 was grown static for 5 days at 30°C to grow pellicles. Pellicles were then removed, washed in sterile  
443 PBS for 10 minutes and imaged. Cell pellets were obtained by digestion of pellicles with 2% sterile  
444 cellulase in PBS (37°C, 250 rpm for 8 hour) before centrifugation at 13,000 rpm and removal of  
445 supernatant. Drying of pellicles was done by placing fresh pellicles on open petri dishes and  
446 incubating at either 30°C (16 hours) or 60°C (3 hours) or by compressing the pellicle and leaving it a  
447 room temperature (24 hours).

448

### 449 **SDS-PAGE and Western Blot**

450 Amyloid associated samples intended for SDS-PAGE analysis were prepared as described previously  
451 (Rouse et al., 2017). Briefly, cell pellets were resuspended in 100  $\mu$ l dH<sub>2</sub>O and lyophilized. Amyloid  
452 containing samples to be monomerised were treated with Formic Acid, frozen and lyophilized a  
453 second time. All samples were resuspended in 8M Urea and loading buffer (2% SDS, 0.2 M Tris-HCl

454 pH 6.8, 0.01% bromophenol blue, 10% glycerol, 2 mM DTT) before heated at 95 °C and separated  
455 on in 12% SDS-PAGE gels. Proteins were transferred by semi-dry Western Blot onto PVDF  
456 membranes visualised with polyclonal antibody and BCIP/NBT (Promega, S3771).

457 Non-amyloid samples were treated with protease inhibitor (Roche complete) before  
458 fractions separated and harvested. Cell fractions were resuspended in loading buffer and heated at  
459 95°C for 10 min. Supernatant fractions were TCA precipitated, washed with acetone, resuspended  
460 in loading buffer and heated at 95°C. Proteins samples were separated on 12-15% SDS-PAGE gels.  
461 Gels were stained with SimplyBlue™ SafeStain (ThermoFisher Scientific) and when required,  
462 transferred by semi-dry Western Blot onto PVDF membranes visualised with polyclonal antibody  
463 and BCIP/NBT (Promega, S3771). Anti-bodies used in this study included a monoclonal  $\alpha$ -his-  
464 antibody (BioLegend, 652502) and polyclonal  $\alpha$ -CsgA-antibody and  $\alpha$ -TasA-antibody.

465

#### 466 **Transmission electron microscopy (TEM)**

467 *E. coli* and *K. rhaeticus* cultures were prepared with 100 nM AHL but further prepared as described  
468 above. Sample Pellets were resuspended in 300  $\mu$ l HEPES buffer (pH 7.5). For *K. rhaeticus* samples  
469 were further treated with 20% cellulase for 4 hrs at 37 °C, before centrifuged again to wash away  
470 excess cellulose and resuspended in 300  $\mu$ l HEPES buffer (pH 7.5). 2  $\mu$ l samples were spotted onto  
471 freshly glow discharged formvar/Carbon on 300 Mesh Nickel grids (Agar Scientific) and blocked for  
472 10 min with BHN1 (1% BSA, 50 mM HEPES, 150 mM NaCl, pH 7.5). Grids were then incubated for 30  
473 min with polyclonal  $\alpha$ -CsgA-antibody (1:10 in BHN1, washed twice with BHN2 (0.1% BSA,  
474 50 mM HEPES, 150 mM NaCl, pH 7.5), incubated with secondary anti-Rabbit IgG-Gold coupled  
475 antibody (1/10 in BHN1) (Anti-Mouse IgG (whole molecule)–Gold antibody produced in goat (Sigma,  
476 G7652), washed twice in BHN2 and HN (50 mM HEPES, 150 mM NaCl, pH 7.5) before stained with  
477 uranyl acetate. The FEI Tecnai G2 Spirit TWIN was used to visualise the cells on the grid.

478

#### 479 **Material Strength Tests**

480 Pellicles were dried flat using a heated press set to 120°C and 1 ton of pressure. Dog bone test  
481 specimens were cut out of the dried cellulose and specimen ends reinforced with card. Dots were  
482 marked on the surface of each specimen for the optical measurement of displacement. Tensile tests  
483 were conducted with a Deben Microtest Tensile Stage. Seven samples were measured per material,  
484 with results normalised for sample thickness.

485

#### 486 **Beta-lactamase Nitrocefin Assay**

487 Beta-lactamase activity was measured using Nitrocefin (Stratech, B6052) as per manufacturer's  
488 instructions. Samples were induced as described above, the extracellular supernatant fraction  
489 removed post centrifugation. Extracellular fractions were equilibrated and diluted in 10x PBS (pH  
490 7.5) at either 1:100 or 1:10 for *E. coli* or *K. rhaeticus* respectively. Beta-lactamase converts nitrocefin  
491 from a yellow to a red substrate and the enzyme activity was calculated as the rate of change of  
492 absorbance (490 nm, Synergy HT plate reader) over the linear region of a graph.

493

#### 494 **Acknowledgements**

495 We are grateful to A. Kan and N. Joshi for the synthetic Curli template, and to the Chapman Lab and Stanley-  
496 Wall Lab for CsgA and TasA-antibodies respectively. The Steve Matthews lab, in particular G. Wu for assisting  
497 with Curli protocols and lyophilisation. The Polizzi lab, in particular R. Aw, and both P. Simpson and T. Pape  
498 at ICL-EM centre. And finally, to Ellis lab members C. Gilbert and W. Shaw for early discussions on Golden  
499 Gate syntax and standards.

500

#### 501 **Funding**

502 We acknowledge the following funders for supporting this work: the UK Engineering and Physical Sciences  
503 Research Council (EPSRC) for grants EP/N026489/1, EP/S032215/1 and studentship project 1846146, the UK  
504 Biotechnology and Biological Sciences Research Council (BBSRC) for training grant BB/R505808/1, the US  
505 Office of Naval Research Global (ONRG) and US Army CDC DEVCOM for grant W911NF-18-1-0387, and the  
506 European CSA on biological standardisation, BIOROBOOST (EU grant number 820699).

507

#### 508 **References**

- 509 Andreou, A.I., Nakayama, N., 2018. Mobius Assembly: A versatile Golden-Gate framework towards  
510 universal DNA assembly. PLoS ONE 13, e0189892. <https://doi.org/10.1371/journal.pone.0189892>
- 511 Assalkhou, R., Balasingham, S., Collins, R.F., Frye, S.A., Davidsen, T., Benam, A.V., Bjoras, M., Derrick, J.P.,  
512 Tonjum, T., 2007. The outer membrane secretin PilQ from *Neisseria meningitidis* binds DNA.  
513 Microbiology 153, 1593–603. <https://doi.org/10.1099/mic.0.2006/004200-0>
- 514 Birnbaum, D.P., Manjula-Basavanna, A., Kan, A., Joshi, N.S., 2020. Hybrid Living Capsules Autonomously  
515 Produced by Engineered Bacteria (preprint). Synthetic Biology.  
516 <https://doi.org/10.1101/2020.11.23.394965>
- 517 Bongers, R.S., Veening, J.-W., Van Wieringen, M., Kuipers, O.P., Kleerebezem, M., 2005. Development and  
518 Characterization of a Subtilin-Regulated Expression System in *Bacillus subtilis*: Strict Control of  
519 Gene Expression by Addition of Subtilin. AEM 71, 8818–8824.  
520 <https://doi.org/10.1128/AEM.71.12.8818-8824.2005>
- 521 Botyanszki, Z., Tay, P.K.R., Nguyen, P.Q., Nussbaumer, M.G., Joshi, N.S., 2015. Engineered catalytic biofilms:  
522 Site-specific enzyme immobilization onto *E. coli* curli nanofibers. Biotechnol. Bioeng. 112, 2016–  
523 2024. <https://doi.org/10.1002/bit.25638>
- 524 Chen, A.Y., Deng, Z., Billings, A.N., Seker, U.O.S., Lu, M.Y., Citorik, R.J., Zakeri, B., Lu, T.K., 2014. Synthesis  
525 and patterning of tunable multiscale materials with engineered cells. Nature Mater 13, 515–523.  
526 <https://doi.org/10.1038/nmat3912>

- 527 Chiasson, D., Giménez-Oya, V., Bircheneder, M., Bachmaier, S., Studtrucker, T., Ryan, J., Sollweck, K.,  
528 Leonhardt, H., Boshart, M., Dietrich, P., Parniske, M., 2019. A unified multi-kingdom Golden Gate  
529 cloning platform. *Sci Rep* 9, 10131. <https://doi.org/10.1038/s41598-019-46171-2>
- 530 Costa, T.R., Felisberto-Rodrigues, C., Meir, A., Prevost, M.S., Redzej, A., Trokter, M., Waksman, G., 2015.  
531 Secretion systems in Gram-negative bacteria: structural and mechanistic insights. *Nat Rev Microbiol*  
532 13, 343–59. <https://doi.org/10.1038/nrmicro3456>
- 533 Durante-Rodríguez, G., de Lorenzo, V., Martínez-García, E., 2014. The Standard European Vector  
534 Architecture (SEVA) Plasmid Toolkit, in: Filloux, A., Ramos, J.-L. (Eds.), *Pseudomonas Methods and*  
535 *Protocols*. Springer New York, New York, NY, pp. 469–478. [https://doi.org/10.1007/978-1-4939-0473-0\\_36](https://doi.org/10.1007/978-1-4939-0473-0_36)
- 536 Engler, C., Youles, M., Gruetzner, R., Ehnert, T.-M., Werner, S., Jones, J.D.G., Patron, N.J., Marillonnet, S.,  
537 2014. A Golden Gate Modular Cloning Toolbox for Plants. *ACS Synth. Biol.* 3, 839–843.  
538 <https://doi.org/10.1021/sb4001504>
- 539 Erskine, E., MacPhee, C.E., Stanley-Wall, N.R., 2018. Functional Amyloid and Other Protein Fibers in the  
540 Biofilm Matrix. *Journal of Molecular Biology* 430, 3642–3656.  
541 <https://doi.org/10.1016/j.jmb.2018.07.026>
- 542 Evans, M.L., Chapman, M.R., 2014. Curli biogenesis: Order out of disorder. *Biochimica et Biophysica Acta*  
543 (BBA) - Molecular Cell Research 1843, 1551–1558. <https://doi.org/10.1016/j.bbamcr.2013.09.010>
- 544 Florea, M., Hagemann, H., Santosa, G., Abbott, J., Micklem, C.N., Spencer-Milnes, X., de Arroyo Garcia, L.,  
545 Paschou, D., Lazenbatt, C., Kong, D., Chughtai, H., Jensen, K., Freemont, P.S., Kitney, R., Reeve, B.,  
546 Ellis, T., 2016. Engineering control of bacterial cellulose production using a genetic toolkit and a  
547 new cellulose-producing strain. *Proceedings of the National Academy of Sciences of the United*  
548 *States of America* 113, E3431-40. <https://doi.org/10.1073/pnas.1522985113>
- 549 Geddes, B.A., Mendoza-Suárez, M.A., Poole, P.S., 2019. A Bacterial Expression Vector Archive (BEVA) for  
550 Flexible Modular Assembly of Golden Gate-Compatible Vectors. *Front. Microbiol.* 9, 3345.  
551 <https://doi.org/10.3389/fmicb.2018.03345>
- 552 Gilbert, C., Ellis, T., 2019. Biological Engineered Living Materials: Growing Functional Materials with  
553 Genetically Programmable Properties. *ACS Synth. Biol.* 8, 1–15.  
554 <https://doi.org/10.1021/acssynbio.8b00423>
- 555 Gilbert, C., Tang, T.-C., Ott, W., Dorr, B.A., Shaw, W.M., Sun, G.L., Lu, T.K., Ellis, T., 2021. Living materials  
556 with programmable functionalities grown from engineered microbial co-cultures. *Nat. Mater.*  
557 <https://doi.org/10.1038/s41563-020-00857-5>
- 558 Gwon, H., Park, K., Chung, S.-C., Kim, R.-H., Kang, J.K., Ji, S.M., Kim, N.-J., Lee, Sunghaeng, Ku, J.-H., Do, E.C.,  
559 Park, S., Kim, M., Shim, W.Y., Rhee, H.S., Kim, J.-Y., Kim, J., Kim, T.Y., Yamaguchi, Y., Iwamuro, R.,  
560 Saito, S., Kim, G., Jung, I.-S., Park, H., Lee, C., Lee, Seungyeon, Jeon, W.S., Jang, W.D., Kim, H.U., Lee,  
561 Sang Yup, Im, D., Doo, S.-G., Lee, Sang Yoon, Lee, H.C., Park, J.H., 2019. A safe and sustainable  
562 bacterial cellulose nanofiber separator for lithium rechargeable batteries. *Proc Natl Acad Sci USA*  
563 201905527. <https://doi.org/10.1073/pnas.1905527116>
- 564 Hernanz-Koers, M., Gandía, M., Garrigues, S., Manzanares, P., Yenush, L., Orzaez, D., Marcos, J.F., 2018.  
565 FungalBraid: A GoldenBraid-based modular cloning platform for the assembly and exchange of DNA  
566 elements tailored to fungal synthetic biology. *Fungal Genetics and Biology* 116, 51–61.  
567 <https://doi.org/10.1016/j.fgb.2018.04.010>
- 568 Hospenthal, M.K., Costa, T.R.D., Waksman, G., 2017. A comprehensive guide to pilus biogenesis in Gram-  
569 negative bacteria. *Nat Rev Microbiol* 15, 365–379. <https://doi.org/10.1038/nrmicro.2017.40>
- 570 Iverson, S.V., Haddock, T.L., Beal, J., Densmore, D.M., 2016. CIDAR MoClo: Improved MoClo Assembly  
571 Standard and New E. coli Part Library Enable Rapid Combinatorial Design for Synthetic and  
572 Traditional Biology. *ACS Synth. Biol.* 5, 99–103. <https://doi.org/10.1021/acssynbio.5b00124>
- 573 Jang, W.D., Hwang, J.H., Kim, H.U., Ryu, J.Y., Lee, S.Y., 2017. Bacterial cellulose as an example product for  
574 sustainable production and consumption. *Microb Biotechnol* 10, 1181–1185.  
575 <https://doi.org/10.1111/1751-7915.12744>
- 576 Kan, A., Birnbaum, D.P., Praveschotinunt, P., Joshi, N.S., 2019. Congo Red Fluorescence for Rapid *In Situ*  
577 Characterization of Synthetic Curli Systems. *Appl Environ Microbiol* 85, e00434-19,  
578 /aem/85/13/AEM.00434-19.atom. <https://doi.org/10.1128/AEM.00434-19>
- 579



- 580 Lee, M.E., DeLoache, W.C., Cervantes, B., Dueber, J.E., 2015. A Highly Characterized Yeast Toolkit for  
581 Modular, Multipart Assembly. *ACS Synth. Biol.* 4, 975–986. <https://doi.org/10.1021/sb500366v>
- 582 Liljeruhm, J., Funk, S.K., Tietscher, S., Edlund, A.D., Jamal, S., Wistrand-Yuen, P., Dyrhage, K., Gynnå, A.,  
583 Ivermark, K., Lövgren, J., Törnblom, V., Virtanen, A., Lundin, E.R., Wistrand-Yuen, E., Forster, A.C.,  
584 2018. Engineering a palette of eukaryotic chromoproteins for bacterial synthetic biology. *J Biol Eng*  
585 12, 8. <https://doi.org/10.1186/s13036-018-0100-0>
- 586 Martella, A., Matjusaitis, M., Auxillos, J., Pollard, S.M., Cai, Y., 2017. EMMA: An Extensible Mammalian  
587 Modular Assembly Toolkit for the Rapid Design and Production of Diverse Expression Vectors. *ACS*  
588 *Synth. Biol.* 6, 1380–1392. <https://doi.org/10.1021/acssynbio.7b00016>
- 589 Mierau, I., Olieman, K., Mond, J., Smid, E.J., 2005. [No title found]. *Microb Cell Fact* 4, 16.  
590 <https://doi.org/10.1186/1475-2859-4-16>
- 591 Moore, S.J., Lai, H.-E., Kelwick, R.J.R., Chee, S.M., Bell, D.J., Polizzi, K.M., Freemont, P.S., 2016. EcoFlex: A  
592 Multifunctional MoClo Kit for *E. coli* Synthetic Biology. *ACS Synth. Biol.* 5, 1059–1069.  
593 <https://doi.org/10.1021/acssynbio.6b00031>
- 594 Nguyen, P.Q., Botyanszki, Z., Tay, P.K.R., Joshi, N.S., 2014. Programmable biofilm-based materials from  
595 engineered curli nanofibres. *Nat Commun* 5, 4945. <https://doi.org/10.1038/ncomms5945>
- 596 Nguyen, P.Q., Courchesne, N.-M.D., Duraj-Thatte, A., Praveschotinunt, P., Joshi, N.S., 2018. Engineered  
597 Living Materials: Prospects and Challenges for Using Biological Systems to Direct the Assembly of  
598 Smart Materials. *Adv. Mater.* 30, 1704847. <https://doi.org/10.1002/adma.201704847>
- 599 Nussbaumer, M.G., Nguyen, P.Q., Tay, P.K.R., Naydich, A., Hysi, E., Botyanszki, Z., Joshi, N.S., 2017.  
600 Bootstrapped Biocatalysis: Biofilm-Derived Materials as Reversibly Functionalizable Multienzyme  
601 Surfaces. *ChemCatChem* 9, 4328–4333. <https://doi.org/10.1002/cctc.201701221>
- 602 Pallach, M., Di Lorenzo, F., Facchini, F.A., Gully, D., Giraud, E., Peri, F., Duda, K.A., Molinaro, A., Silipo, A.,  
603 2018. Structure and inflammatory activity of the LPS isolated from *Acetobacter pasteurianus*  
604 CIP103108. *Int J Biol Macromol* 119, 1027–1035. <https://doi.org/10.1016/j.ijbiomac.2018.08.035>
- 605 Roberts, S., Dzuricky, M., Chilkoti, A., 2015. Elastin-like polypeptides as models of intrinsically disordered  
606 proteins. *FEBS Letters* 589, 2477–2486. <https://doi.org/10.1016/j.febslet.2015.08.029>
- 607 Rouse, S.L., Hawthorne, W.J., Berry, J.L., Chorev, D.S., Ionescu, S.A., Lambert, S., Stylianou, F., Ewert, W.,  
608 Mackie, U., Morgan, R.M.L., Otzen, D., Herbst, F.A., Nielsen, P.H., Dueholm, M., Bayley, H.,  
609 Robinson, C.V., Hare, S., Matthews, S., 2017. A new class of hybrid secretion system is employed in  
610 *Pseudomonas amyloid* biogenesis. *Nat Commun* 8, 263. [https://doi.org/10.1038/s41467-017-](https://doi.org/10.1038/s41467-017-00361-6)  
611 00361-6
- 612 Salis, H.M., Mirsky, E.A., Voigt, C.A., 2009. Automated design of synthetic ribosome binding sites to control  
613 protein expression. *Nat Biotechnol* 27, 946–950. <https://doi.org/10.1038/nbt.1568>
- 614 Seker, U.O.S., Chen, A.Y., Citorik, R.J., Lu, T.K., 2017. Synthetic Biogenesis of Bacterial Amyloid  
615 Nanomaterials with Tunable Inorganic-Organic Interfaces and Electrical Conductivity. *ACS Synth*  
616 *Biol* 6, 266–275. <https://doi.org/10.1021/acssynbio.6b00166>
- 617 Singh, A., Walker, K.T., Ledesma-Amaro, R., Ellis, T., 2020. Engineering Bacterial Cellulose by Synthetic  
618 Biology. *IJMS* 21, 9185. <https://doi.org/10.3390/ijms21239185>
- 619 Sivanathan, V., Hochschild, A., 2012. Generating extracellular amyloid aggregates using *E. coli* cells. *Genes*  
620 *Dev.* 26, 2659–2667. <https://doi.org/10.1101/gad.205310.112>
- 621 Tabor, S., 1990. Expression Using the T7 RNA Polymerase/Promoter System. *Current Protocols in Molecular*  
622 *Biology* 11. <https://doi.org/10.1002/0471142727.mb1602s11>
- 623 Tang, T.-C., An, B., Huang, Y., Vasikaran, S., Wang, Y., Jiang, X., Lu, T.K., Zhong, C., 2020. Materials design by  
624 synthetic biology. *Nat Rev Mater.* <https://doi.org/10.1038/s41578-020-00265-w>
- 625 Tay, P.K.R., Nguyen, P.Q., Joshi, N.S., 2017. A Synthetic Circuit for Mercury Bioremediation Using Self-  
626 Assembling Functional Amyloids. *ACS Synth. Biol.* 6, 1841–1850.  
627 <https://doi.org/10.1021/acssynbio.7b00137>
- 628 Teh, M.Y., Ooi, K.H., Danny Teo, S.X., Bin Mansoor, M.E., Shaun Lim, W.Z., Tan, M.H., 2019. An Expanded  
629 Synthetic Biology Toolkit for Gene Expression Control in *Acetobacteraceae*. *ACS Synth Biol* 8, 708–  
630 723. <https://doi.org/10.1021/acssynbio.8b00168>
- 631 Valenzuela-Ortega, M., French, C., 2019. Joint Universal Modular Plasmids (JUMP): A flexible and  
632 comprehensive platform for synthetic biology. *bioRxiv* 799585. <https://doi.org/10.1101/799585>



- 633 Van Gerven, N., Goyal, P., Vandenbussche, G., De Kerpel, M., Jonckheere, W., De Greve, H., Remaut, H.,  
634 2014. Secretion and functional display of fusion proteins through the curli biogenesis pathway.  
635 *Molecular microbiology* 91, 1022–35. <https://doi.org/10.1111/mmi.12515>
- 636 Van Gerven, N., Klein, R.D., Hultgren, S.J., Remaut, H., 2015. Bacterial amyloid formation: structural insights  
637 into curli biogenesis. *Trends in microbiology* 23, 693–706. <https://doi.org/10.1016/j.tim.2015.07.010>
- 638 Vasudevan, R., Gale, G.A.R., Schiavon, A.A., Puzorjov, A., Malin, J., Gillespie, M.D., Vavitsas, K., Zulkower, V.,  
639 Wang, B., Howe, C.J., Lea-Smith, D.J., McCormick, A.J., 2019. CyanoGate: A Modular Cloning Suite  
640 for Engineering Cyanobacteria Based on the Plant MoClo Syntax. *Plant Physiol.* 180, 39.  
641 <https://doi.org/10.1104/pp.18.01401>
- 642 Walker, K.T., Goosens, V.J., Das, A., Graham, A.E., Ellis, T., 2018. Engineered cell-to-cell signalling within  
643 growing bacterial cellulose pellicles. *Microb Biotechnol.* <https://doi.org/10.1111/1751-7915.13340>
- 644 Wang, M., Huang, M., Zhang, J., Ma, Y., Li, S., Wang, J., 2017. A novel secretion and online-cleavage strategy  
645 for production of cecropin A in *Escherichia coli*. *Scientific Reports* 7, 7368.  
646 <https://doi.org/10.1038/s41598-017-07411-5>
- 647 Weber, E., Engler, C., Gruetzner, R., Werner, S., Marillonnet, S., 2011. A modular cloning system for  
648 standardized assembly of multigene constructs. *PLoS one* 6, e16765.  
649 <https://doi.org/10.1371/journal.pone.0016765>
- 650 Wicke, N., Radford, D., Verrone, V., Wipat, A., French, C.E., 2017. BacilloFlex: A modular DNA assembly  
651 toolkit for *Bacillus subtilis* synthetic biology (preprint). *Synthetic Biology*.  
652 <https://doi.org/10.1101/185108>
- 653 Wu, D., Schandry, N., Lahaye, T., 2018. A modular toolbox for Golden-Gate-based plasmid assembly  
654 streamlines the generation of *Ralstonia solanacearum* species complex knockout strains and multi-  
655 cassette complementation constructs: A Golden-Gate toolkit for the *Rssc*. *Molecular Plant*  
656 *Pathology* 19, 1511–1522. <https://doi.org/10.1111/mpp.12632>
- 657 Yadav, V., Paniliatis, B.J., Shi, H., Lee, K., Cebe, P., Kaplan, D.L., 2010. Novel in vivo-degradable cellulose-  
658 chitin copolymer from metabolically engineered *Gluconacetobacter xylinus*. *Appl Environ Microbiol*  
659 76, 6257–65. <https://doi.org/10.1128/AEM.00698-10>
- 660 Zhong, C., Gurry, T., Cheng, A.A., Downey, J., Deng, Z., Stultz, C.M., Lu, T.K., 2014. Strong underwater  
661 adhesives made by self-assembling multi-protein nanofibres. *Nat Nanotechnol* 9, 858–866.  
662 <https://doi.org/10.1038/nnano.2014.199>
- 663